The 9th European Congress on Computational Methods in Applied Sciences and Engineering
ECCOMAS Congress 2024
3–7 June 2024, Lisboa, Portugal

A MODEL-REDUCTION TECHNIQUE BASED ON PERTURBATION METHOD FOR THE ANALYSIS OF VARIABLE-STIFFNESS SHELLS

C.A. YAN[1] AND R. VESCOVINI[1]

[1] Dipartimento di Scienze e Tecnologie Aerospaziali (DAER)
Politecnico di Milano
Via La Masa 34, 20156, Milan, Italy
e-mail: chengangelo.yan@polimi.it, riccardo.vescovini@polimi.it

Key words: Variable-stiffness composite, Shell structures, Postbuckling analysis, Finite element method, Rayleigh-Ritz technique, Perturbation approach

Summary. This paper explores a novel approach that combines the *ps*-version of the Finite Element Method (*ps*-FEM), the Rayleigh-Ritz Method (RRM), and the Asymptotic-Numerical Method (ANM) to realize an effective Model Reduction Technique (MRT). The study shows that a proper refinement of the finite element model and selection of Ritz basis vectors leads to efficient, yet accurate, Reduced-Order Models (ROMs). Numerical tests give evidence of the approach's validity in postbuckling problems of Variable-Stiffness (VS) panels. Comparisons with high-fidelity Abaqus simulations demonstrate the potential of the present framework as a valuable tool for the analysis and design of new-generation VS structures.

1 INTRODUCTION

The analysis and design of Variable-Stiffness (VS) plates and shells have gained considerable attention in recent times for their improved performances over classical laminates. However, modeling these innovative configurations demands refined numerical models to capture the complex elastic couplings at different scale levels, from global to local. Moreover, the solution of such models can be computationally challenging, especially for composite structures exhibiting highly nonlinear response.

Over the years, different strategies have been proposed to combine modeling fidelity and reduced computational times. For instance, refined composite shell theories [1, 2, 3], efficient numerical methods [4, 5], and rapid solution procedures [6, 7, 8] have been proposed as viable strategies.

One promising approach to realize fast and reliable simulation strategies is represented by Model Reduction Techniques (MRTs). The underlying idea consists in replacing the Full-Order Model (FOM) with a Reduced-Order Model (ROM), which features the main physical characteristics of the problem at hand, but with a much lower dimensionality.

In the context of static nonlinear analysis, different approaches have been proposed to perform this condensation. In [9] a superposition of linear buckling modes is employed to approximate the nonlinear solution of the FOM. Another possible method relies upon the combination of the linear solution and its iterative vector corrections [10]. A MRT has been proposed in [11] where the FOM solution is represented as a linear combination of the high-order derivative vectors

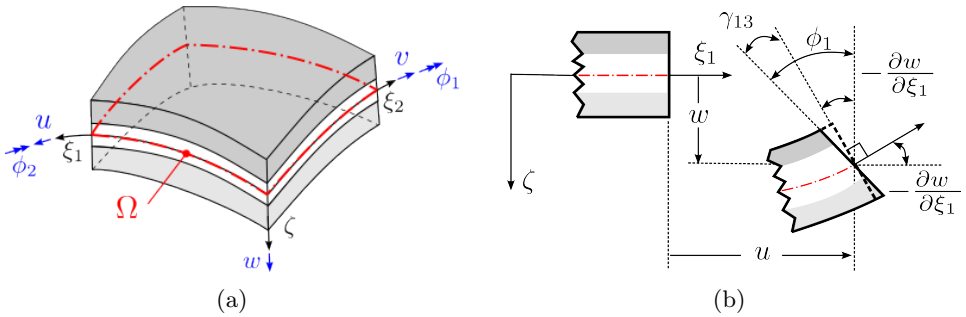

Figure 1: Shell mathematical model: (a) reference system and (b) kinematics.

used in perturbation techniques. The approach proposed in [12] involves the use of nonlinear solution vectors together with the correction vectors generated during the iterative procedure. Superposition of nonlinear deformation modes at successive incremental steps have also been employed to generate ROMs in [13]. The work of [14] explores the hybrid use of linear buckling modes, path derivative modes and deformation modes to construct ROMs.

The Koiter's perturbation method can also be viewed as a MRT where the ROM is generated in the form of a quadratic asymptotic expansion. In this context, MRT based on perturbation approaches have been recently the focus of attention for the analysis of VS structures due to their effectiveness in solving nonlinear problems. In [15], a perturbation method is implemented in the DIANA finite element code and is employed to study the initial postbuckling response of VS plates. A hybrid Koiter-Newton approach [16] has been recently developed in a FE framework to trace the equilibrium curves of VS shells in their "*deep*" postbuckling regime.

The present work aims at extending the current state-of-the-art through a new approach which combines: an efficient Finite Element method – the *ps*-version of the Finite Element Method (*ps*-FEM) [17, 18, 19] –, an effective reduction technique based on the Rayleigh-Ritz Method (RRM) [11], and a fast asymptotic solution procedure, known as the Asymptotic-Numerical Method (ANM) [20].

2 GOVERNING EQUATIONS

The kinematics of the shell is described using the First-order Shear Deformation Theory (FSDT), so that the displacement field is represented in terms of the displacements $\{u, v, w\}^{\mathrm{T}}$ and rotations $\{\phi_1, \phi_2\}^{\mathrm{T}}$ components on the shell's middle surface Ω. A sketch is reported in Figure 1

The governing equations are obtained starting from the Total Potential Energy (TPE)

$$\Pi(\mathbf{u}, \lambda) = \frac{1}{2} \int_{\Omega} \left(\epsilon^{0\mathrm{T}} \mathbf{A} \epsilon^{0} + \mathbf{k}^{\mathrm{T}} \mathbf{D} \mathbf{k} + 2\epsilon^{0\mathrm{T}} \mathbf{B} \mathbf{k} + \gamma^{0\mathrm{T}} \overline{\mathbf{A}} \gamma^{0} \right) \mathrm{d}\Omega + \lambda V(\mathbf{u}), \tag{1}$$

where the vectors $\boldsymbol{\epsilon}^0$, $\mathbf{k}$, $\boldsymbol{\gamma}^0$ are the generalized strains and curvatures, $\mathbf{A}, \mathbf{B}, \mathbf{D}, \overline{\mathbf{A}}$ are the matrices defining the shell constitutive law, while $V(\mathbf{u})$ is the potential of the applied loads, proportional to the scaling factor λ.

The TPE is a quartic function of the generalized displacements $\mathbf{u} = \{u, v, w, \phi_1, \phi_2\}^{\mathrm{T}}$. Consequently, its variation $\delta\Pi = 0$ leads to a set of equilibrium equations with cubic nonlinearities

$$l(\mathbf{u}) + q(\mathbf{u}, \mathbf{u}) + c(\mathbf{u}, \mathbf{u}, \mathbf{u}) = \lambda f, \tag{2}$$

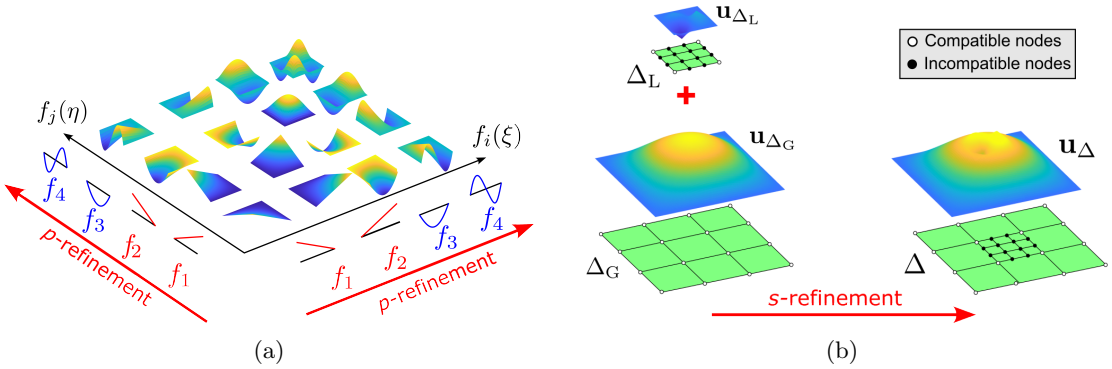

Figure 2: Construction and refinement of the finite element (a) polynomial space, and (b) mesh.

where $l(\cdot)$, $q(\cdot,\cdot)$ and $c(\cdot,\cdot,\cdot)$ are operators obtained from the variation of the quadratic, cubic and quartic part of the TPE, respectively; the operator f is specified according to the loading conditions considered.

The variational problem in Eq. (2) can be discretized using different numerical methods, such as Finite Elements (FEs).

3 FINITE ELEMENT DISCRETIZATION

This work adopts an advanced spatial discretization called the *ps*-version of the Finite Element Method (*ps*-FEM) [18]. Within this FE scheme, quasi-optimal numerical models can be generated by adjusting the elements' order and size in accordance with the smoothness characteristics of the solution. This is achieved through application of different refinement strategies [17], i.e. *p*-refinement, *s*-refinement, or a combinations of the twos, see Figure 2.

In the *ps*-FEM, the polynomial space is constructed from the set of one-dimensional hierarchical functions [22]

$$f_1(\xi) = \frac{1}{2}(1+\xi), \quad f_2(\xi) = \frac{1}{2}(1-\xi), \quad f_{i+1}(\xi) = \sqrt{\frac{2i-1}{2}}\int_{-1}^{\xi} P_{i-1}(\xi)d\xi \quad \text{for} \quad i>2, \tag{3}$$

where $P_k(\xi)$ defines the Legendre polynomial of order k. The resulting two-dimensional polynomial space (Figure 2(a)) has the advantage of being quasi-orthogonal and hierarchical. As result, the FE matrices remain well-conditioned even for very high polynomial orders, and the refinement of the series can be performed easily, with no need of reassembling the whole FE system.

The mesh is constructed using the concept of "*refine-by-superposition*" [23], so that the FE approximation is decomposed into two parts, one described by a global mesh Δ_G and the second one by a local mesh Δ_L. So:

$$\mathbf{u} \simeq \mathbf{u}_\Delta = \begin{cases} \mathbf{u}_{\Delta_G} & \text{in} \quad \Omega - \Omega_L \\ \mathbf{u}_{\Delta_G} + \mathbf{u}_{\Delta_L} & \text{in} \quad \Omega_L \end{cases},$$

where $\mathbf{u}_{\Delta_G}$ is the global mesh solution defined in Ω, while $\mathbf{u}_{\Delta_L}$ is the local mesh solution defined in $\Omega_L \subset \Omega$ (Figure 2(b)). The possibility of overlaying incompatible mesh discretizations provides

a high level of flexibility when performing local mesh refinements, as no transition regions or multi-point constraints are required.

After introducing the FE approximation, the continuous problem of Eq. (2) turns into

$$\mathbf{r}(\mathbf{c},\lambda) = \mathbf{L}\mathbf{c} + \mathbf{Q}(\mathbf{c})\mathbf{c} + \mathbf{C}(\mathbf{c},\mathbf{c})\mathbf{c} - \lambda\mathbf{f} = 0 \quad \text{with} \quad \mathbf{c} \in \mathbf{R}^{N\times 1}, \tag{4}$$

where N is the dimension of the FE model, $\mathbf{L} \in \mathbf{R}^{N\times N}$ is the the linear stiffness matrix, $\mathbf{f} \in \mathbf{R}^{N\times 1}$ is the vector of external loads, while $\mathbf{Q} \in \mathbf{R}^{N\times N\times N}$ and $\mathbf{C} \in \mathbf{R}^{N\times N\times N\times N}$ are tensors of order three and four obtained from the cubic and quartic terms of the TPE, respectively.

The *ps*-FEM enables the generation of extremely efficient numerical models, where relatively few DOFs suffice to guarantee accurate results. Despite these interesting features, the nonlinear solution procedure can be still computationally intensive. For instance, in the presence of strong nonlinearities, classical Iterative-Incremental Procedures (IIPs) may require a large number of matrix factorizations and residual evaluations. The cost of these operations increases quickly with the size of the FE model.

To address this issue, we propose a Model Reduction Technique (MRT) to further improve the effectiveness of the *ps*-FE model in a static nonlinear environment.

4 MODEL REDUCTION TECHNIQUE

Model Reduction Techniques (MRTs) are procedures for reducing a large-size problem, i.e. the Full-Order Model (FOM), into a smaller substitute, or the Reduced-Order Model (ROM). These procedures are based on two main steps: (I) generation of a reduced-basis subspace of global approximation vectors, and (II) projection of the original problem onto the lower-dimensional subspace.

The MRT proposed in this work employs a perturbation procedure for generating the reduced-basis subspace, while the projection is carried out through the Rayleigh-Ritz Method (RRM).

4.1 Generation of the subspace

The reduced-basis subspace $\mathbf{V}$ is generated using a perturbation procedure known as the Asymptotic-Numerical Method (ANM) [20]. In the present study, the ANM is employed to generate two different subspaces, i.e. one based on the path derivatives of static modes $\mathbf{V}_\mathrm{S}$, while the second one based on the path derivatives of buckling modes $\mathbf{V}_\mathrm{B}$.

Subspace 1: Static modes
The path derivatives of a generic static mode $\mathbf{c}_\mathrm{S}$ in equilibrium at load level λ_S are generated from the solution of a series of linear algebraic problems [24]

$$\begin{aligned} k=1: &\qquad \mathbf{T}_\mathrm{S}\mathbf{c}_1 = \lambda_1\mathbf{f} &&\text{and} &&\lambda_1 = 1, \\ k=n: &\qquad \mathbf{T}_\mathrm{S}\mathbf{c}_n = \lambda_n\mathbf{f} - \mathbf{q}_n &&\text{and} &&\lambda_n = \mathbf{c}_1^\mathrm{T}\mathbf{q}_n/\mathbf{c}_1^\mathrm{T}\mathbf{f}, \end{aligned} \tag{5}$$

where $\mathbf{c}_k$ represents the k-th path derivative, $\mathbf{T}_\mathrm{S}$ is the tangent stiffness matrix evaluated at $\mathbf{c}_\mathrm{S}$, while $\mathbf{q}_k$ is a vector of the nonlinear terms

$$\mathbf{q}_k = \sum_{r=1}^{k-1} \mathbf{Q}(\mathbf{c}_r)\mathbf{c}_{k-r} + \sum_{r=1}^{k-1} \mathbf{C}(\mathbf{c}_0, \mathbf{c}_r)\mathbf{c}_{k-r} + \sum_{r=1}^{k-1} \mathbf{C}(\mathbf{c}_r, \mathbf{c}_0)\mathbf{c}_{k-r} + \sum_{r=1}^{k-1} \mathbf{C}(\mathbf{c}_r, \mathbf{c}_{k-r})\mathbf{c}_0 + \\ + \sum_{r=1}^{k-1}\sum_{q=1}^{r-1} \mathbf{C}(\mathbf{c}_q, \mathbf{c}_{k-r})\mathbf{c}_{r-q}. \tag{6}$$

The procedure outlined in Eq. (5) allows for the generation of a subspace of approximation vectors with low computational effort. Indeed, it relies on a sequence of linear problems sharing the same coefficient matrix $\mathbf{T}_\mathrm{S}$. Moreover, the approach can be automatized to generate an arbitrary number of vector elements

$$\mathbf{V}_\mathrm{S} = [\mathbf{c}_\mathrm{S}, \mathbf{c}_1, ..., \mathbf{c}_n] \in \mathbf{R}^{N\times n}, \tag{7}$$

where n is the size of the base.

Subspace 2: Buckling modes
The path derivatives of the buckling mode $\mathbf{c}_\mathrm{B}$ with bifurcation multiplier λ_B are obtained from [24]

$$\begin{aligned} k=1: &\qquad [\mathbf{L} + \lambda_\mathrm{B}\mathbf{G}_0]\,\hat{\mathbf{c}}_1 = 0 \qquad \text{and} \qquad \hat{\lambda_1} = -\left[\hat{\mathbf{c}}_1^\mathrm{T}\hat{\mathbf{q}}_2\right] / \left[\hat{\mathbf{c}}_1^\mathrm{T}\mathbf{G}_0\hat{\mathbf{c}}_1\right], \\ k=n: &\qquad \mathbf{T}_\mathrm{B}\hat{\mathbf{c}}_n = -\hat{\mathbf{q}}_n - \hat{\mathbf{g}}_n \qquad \text{and} \qquad \hat{\lambda}_n = -\left[\hat{\mathbf{c}}_1^\mathrm{T}\hat{\mathbf{g}}_n + \hat{\mathbf{c}}_1^\mathrm{T}\hat{\mathbf{q}}_{n+1}\right] / \left[\hat{\mathbf{c}}_1^\mathrm{T}\mathbf{G}_0\hat{\mathbf{c}}_1\right], \end{aligned} \tag{8}$$

where $\mathbf{G}_0$ is the geometric stiffness matrix evaluated at the prebukling condition $\mathbf{c}_0$, $\mathbf{T}_\mathrm{B}$ is the tangent stiffness matrix evaluated at the bifurcation point, while the forcing term $\hat{\mathbf{g}}_k$ is

$$\hat{\mathbf{g}}_k = \sum_{r=1}^{k-1} \hat{\lambda}_r \mathbf{G}_0 \hat{\mathbf{c}}_{r-k}. \tag{9}$$

Similarly to the procedure presented for static modes, Eq. (8) provides an efficient and easy procedure for generating a reduced-basis subspace of arbitrary dimension n

$$\mathbf{V}_\mathrm{B} = [\mathbf{c}_0, \hat{\mathbf{c}}_1, ..., \hat{\mathbf{c}}_n] \in \mathbf{R}^{N\times n} \tag{10}$$

where $\hat{\mathbf{c}}_1 = k\mathbf{c}_\mathrm{B}$ is a multiple of the buckling mode obtained from the solution of a linear eigenvalue problem – first of Eq. (8) –, while $\hat{\mathbf{c}}_k$ denotes the path derivatives available from the solution of a sequence of linear algebraic problems – second of Eq. (8). More details on the solution procedure are presented in [24].

4.2 Projection on the subspace

The Rayleigh-Ritz method is employed to project the governing equations of the FOM onto the reduced subspace. The basis vectors composing the subspace are used as trial functions to approximate the solution of the FOM

$$\mathbf{c} = \mathbf{V}\boldsymbol{\psi} \quad \text{and} \quad \delta\mathbf{c} = \mathbf{V}\delta\boldsymbol{\psi}, \tag{11}$$

where $\boldsymbol{\psi}$ is the vector of Ritz coefficients, while $\mathbf{V}$ is a matrix of global approximation vectors, or Ritz basis vectors, obtained either from Eq. (7) or Eq. (10).

The projection of Eq. (4) onto the subspace $\mathbf{V}$, i.e.

$$\delta\boldsymbol{\psi}^{\mathrm{T}}\mathbf{V}^{\mathrm{T}}\mathbf{r}(\mathbf{V}\boldsymbol{\psi},\lambda)=0, \tag{12}$$

gives a set of reduced governing equations

$$\mathbf{r}^{*}(\boldsymbol{\psi},\lambda)=\mathbf{L}^{*}\boldsymbol{\psi}+\mathbf{Q}^{*}(\boldsymbol{\psi})\boldsymbol{\psi}+\mathbf{C}^{*}(\boldsymbol{\psi},\boldsymbol{\psi})\boldsymbol{\psi}-\lambda\mathbf{f}^{*}=0 \quad \text{with} \quad \boldsymbol{\psi}\in\mathbf{R}^{n\times 1}. \tag{13}$$

The coefficients defining the ROM, $\mathbf{L}^{*}$, $\mathbf{Q}^{*}$, $\mathbf{C}^{*}$ and $\mathbf{f}^{*}$, are given as

$$L^{*}_{ij}=\mathbf{c}_i^{\mathrm{T}}\mathbf{L}\mathbf{c}_j, \quad Q^{*}_{ijk}=\mathbf{c}_i^{\mathrm{T}}\mathbf{Q}(\mathbf{c}_j)\mathbf{c}_k, \quad C^{*}_{ijkl}=\mathbf{c}_i^{\mathrm{T}}\mathbf{C}(\mathbf{c}_j,\mathbf{c}_k)\mathbf{c}_l, \quad f^{*}_{i}=\mathbf{c}_i^{\mathrm{T}}\mathbf{f}, \tag{14}$$

where $\mathbf{c}_i$ is the generic i-th column element of $\mathbf{V}$.

The set of Eq. (13) represents the governing equations of the ROM, whose size is much smaller than the FOM, i.e. $n << N$. Rather than solving this set of nonlinear discrete equations via standard IIPs, we propose a strategy based on a perturbation approach.

5 PERTURBATION SOLUTION PROCEDURE

In this section, the ANM is employed for solving the ROM described by Eq. (13). According to this approach, the solution $(\boldsymbol{\psi},\lambda)$ is approximated with a truncated expansion series around a known initial solution $(\boldsymbol{\psi}_0,\lambda_0)$

$$\boldsymbol{\psi}(\xi)=\boldsymbol{\psi}_0+\sum_{k=1}^{n}\xi^{k}\boldsymbol{\psi}_k \quad \text{and} \quad \lambda(\xi)=\lambda_0+\sum_{k=1}^{n}\xi^{k}\lambda_k, \tag{15}$$

where n is the truncation order and ξ is an expansion parameter, here taken as the arclength measure [20].

Substituting Eq. (15) into Eq. (13) and collecting power-like terms in ξ^k, the initial reduced nonlinear problem is decomposed into a series of linear ones

$$\begin{aligned}
&k=1: && \mathbf{T}_0^{*}\boldsymbol{\psi}_1=\lambda_1\mathbf{f}^{*} && \text{and} && \boldsymbol{\psi}_1^{\mathrm{T}}\boldsymbol{\psi}_1+\lambda_1\lambda_1=1,\\
&k=n: && \mathbf{T}_0^{*}\boldsymbol{\psi}_n=\lambda_n\mathbf{f}^{*}-\mathbf{q}_n^{*} && \text{and} && \boldsymbol{\psi}_1^{\mathrm{T}}\boldsymbol{\psi}_n+\lambda_1\lambda_n=0,
\end{aligned} \tag{16}$$

where $\mathbf{T}_0^{*}$ is the tangent matrix of the ROM evaluated at $\boldsymbol{\psi}_0$, while the vector $\mathbf{q}_k^{*}$ is assembled according to Eq. (6). The linear problems are solved using the procedure presented in [20]. In particular

$$k=1: \qquad \hat{\boldsymbol{\psi}}_1=\mathbf{T}_0^{*-1}\mathbf{f}^{*}, \qquad \lambda_1=\frac{1}{\sqrt{1+\hat{\boldsymbol{\psi}}_1^{\mathrm{T}}\hat{\boldsymbol{\psi}}_1}}, \qquad \boldsymbol{\psi}_1=\lambda_1\hat{\boldsymbol{\psi}}_1, \tag{17}$$

$$k=n: \qquad \hat{\boldsymbol{\psi}}_k=\mathbf{T}_0^{*-1}\mathbf{q}_k^{*}, \qquad \lambda_k=-\boldsymbol{\psi}_1^{\mathrm{T}}\hat{\boldsymbol{\psi}}_k\lambda_1, \qquad \boldsymbol{\psi}_k=\frac{\lambda_k}{\lambda_1}\boldsymbol{\psi}_1+\hat{\boldsymbol{\psi}}_k. \tag{18}$$

The main advantage of the ANM over IIPs is that the solution in available analytically in terms of a power series, see Eq. (15), and not in a "*point-by-point*" fashion. Moreover, the computational cost is drastically reduced as one single matrix inversion is necessary for the definition of the terms of the series, i.e. $(\boldsymbol{\psi}_k,\lambda_k)$.

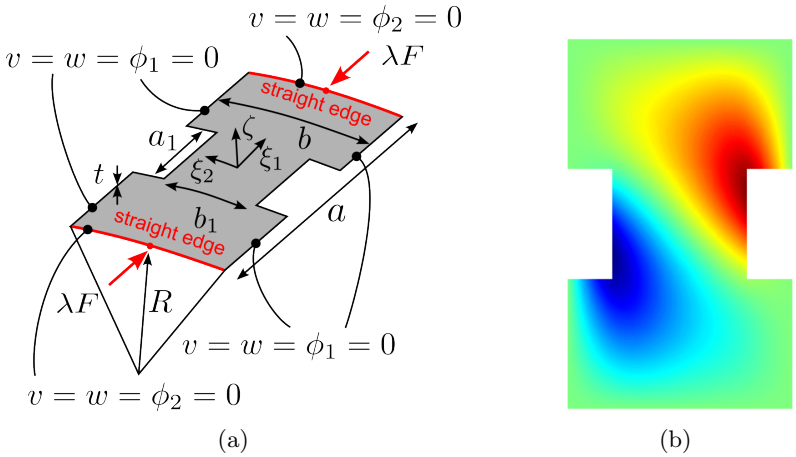

Figure 3: Benchmark description: (a) geometry with boundary/loading conditions, and (b) imperfection shape.

6 RESULTS

In this section, the main features of the proposed computational framework are illustrated with a numerical example.

The structure under investigation is illustrated in Figure 3(a), and consists of a composite panel with cylindrical curvature loaded with a compressive load. In the analysis, an initial imperfection is introduced with the shape of the first buckling mode and a maximum amplitude-to-thickness ratio of 0.5. The contour of the imperfection is reported in Figure 3(b). The geometric and material data are summarized in Tables 1 and 2, respectively.

Table 1: Geometric data for the shell.

a (mm)	b (mm)	a_1 (mm)	b_1 (mm)	R (mm)	t (mm)
200	100	60	60	500	1

Table 2: Material properties considered for the laminate.

E_{11} (MPa)	E_{22} (MPa)	G_{12} (MPa)	G_{13} (MPa)	G_{23} (MPa)	ν_{12} (-)	ν_{13} (-)	ν_{23} (-)
369,000	5,030	5,240	5,240	5,240	0.31	0.31	0.31

There are two main features to be noted for the test case at hand. Firstly, the shell has a complex geometry with re-entrant edges and free-edge boundary conditions. These are sources of stress concentrations, so appropriate numerical grids are needed. Secondly, the material is characterized by an (artificially) high orthotropy ratio $E_{11}/E_{22} > 70$. This aspect, together with the Variable-Stiffness lay-up $[90 \pm \langle 30, 0 \rangle]_{2s}$, promotes complex elastic couplings, hence potential difficulties in the convergence of the solution [21]. Furthermore, the response of the shell exhibits an unstable postbuckling response with snap-through and snap-back occurring

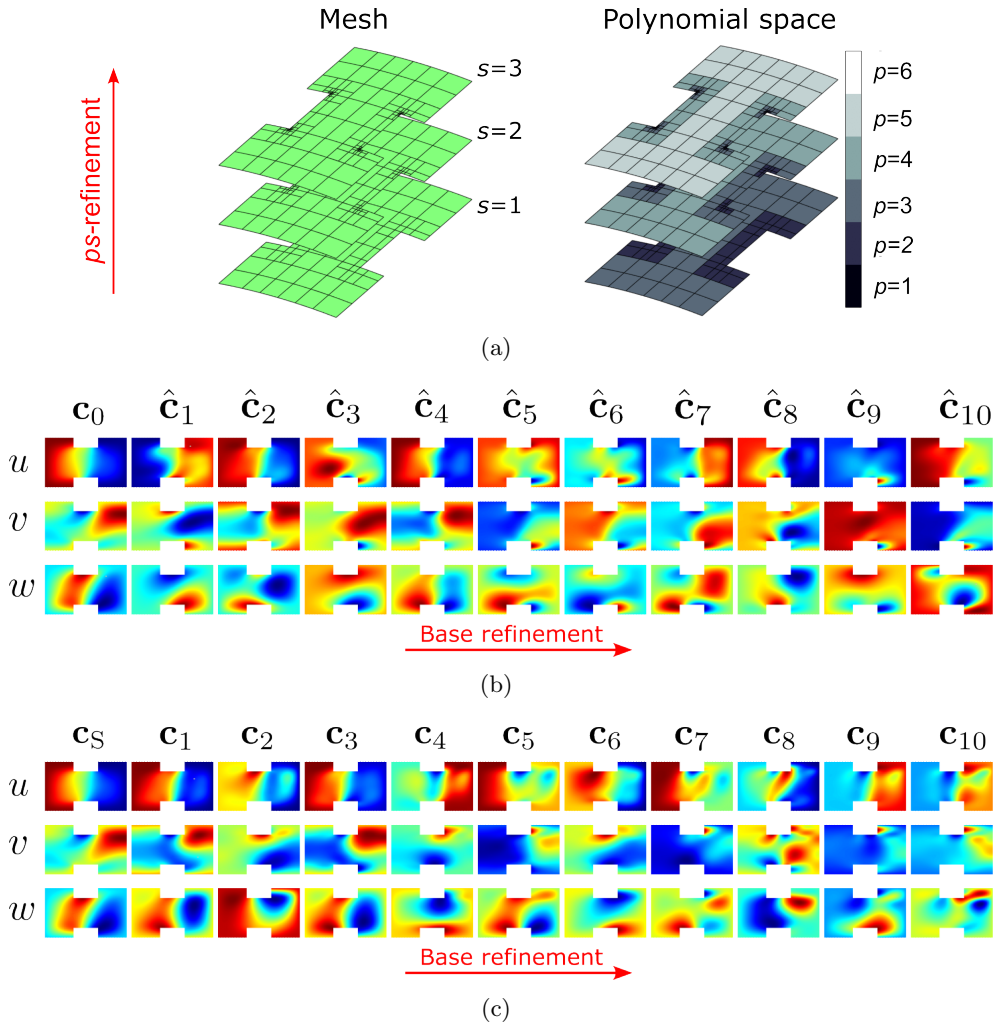

Figure 4: Numerical models employed for the solution of the benchmark problem: (a) FOM$_{ps}$, (b) ROM$_{\mathrm{B}}$, and (c) ROM$_{\mathrm{S}}$.

along the equilibrium path.

The problem is solved by considering three different numerical models, here denoted as FOM$_{ps}$, ROM$_{\mathrm{B}}$ and ROM$_{\mathrm{S}}$. The features of these three models are summarized in Figure 4. The first one is the full *ps*-FE model, while the models ROM$_{\mathrm{B}}$ and ROM$_{\mathrm{S}}$ are ROMs generated with the path derivatives of buckling and static modes, respectively.

For all models, the solution is obtained using the ANM and is expressed in terms of load versus end-shortening curves in Figure 5.

6.1 Solution with the FOM

The full *ps*-FE model is illustrated in Figure 4(a). It is based on a global/coarse mesh with 44 elements, further refined with 4 local/finer meshes at the internal corners, where localized effects are promoted by the shell geometry.

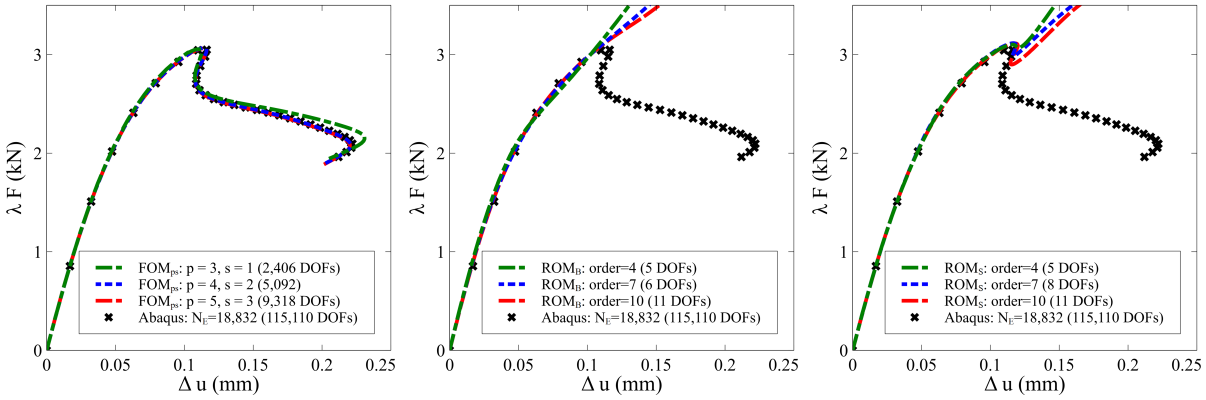

Figure 5: Load vs end-shortening curves from the solution of the (a) FOM$_{ps}$, (b) ROM$_\mathrm{B}$, and (c) ROM$_\mathrm{S}$.

The load-shortening curves obtained via FOM$_{ps}$ are reported in Figure 5(a) for different levels of *ps*-refinements. The sequence of refinement is carried out such that large-size/high-order elements are employed in the regions where the solution is smooth, while small-size/low-order elements in regions of local stress concentrations.

The results are compared with high fidelity Abaqus simulations based on a FE model with 18,832 elements (115,110 DOFs). As shown in Figure 5(a), the FOM$_{ps}$ leads to converged results with 9,318 DOFs, consisting in a saving of 92% in DOFs with respect to the Abaqus model. This is achieved without any loss of accuracy thanks to the advanced refinements strategy proper of the *ps*-FEM.

6.2 Solution with ROM based on buckling modes

The first ROM is constructed using the path derivatives of the first buckling mode, see Figure 4(b). The path derivatives are generated via Eq. (10) using a nonlinear prebuckling condition $\mathbf{c}_0$ corresponding to the load level of 2.95 kN.

The results are illustrated in Figure 5(b) for models generated with different number of path derivatives. The comparison is presented with Abaqus results. As shown, a considerable portion of the nonlinear prebuckling field is captured very well if 10 path derivatives are used.

The solution of ROM$_\mathrm{B}$ is almost instantaneous, and just few seconds are required. Indeed, the combination of the ROM's lower dimensionality – 11 DOFs in this case – and the ANM-based solution method results in an effective solution strategy. It is worth noting that the ROM$_\mathrm{B}$ model fails in predicting the limit point of the shell. So, the subspace employed $\mathbf{V}_\mathrm{B}$ can be successfully applied for the prediction of the nonlinear prebuckling field, but not for the postbuckling response.

6.3 Solution with ROM based on static modes

A different ROM is proposed in this section based on the path derivatives of the static mode in equilibrium at the load level of 2.95 kN, see Figure 4(c). The results are illustrated in Figure 5(c). They demonstrate that the ROM$_\mathrm{S}$ provides an improved representation of the equilibrium path with respect to the ROM$_\mathrm{B}$. In this case, the limit load is accurately predicted, and just 4 path

derivatives of the static mode are sufficient for this purpose.

On the other hand, the description of the postbuckling field is more challenging. The simplest model with 4 path derivatives does not capture the descending part of the equilibrium curve. By expanding the subspace up to the 10^{th} path derivative, a satisfactory prediction is obtained for the initial portion of the curve. However, if the deep postbuckling response is of concern, other strategies are necessary.

7 CONCLUSIONS

The present work has introduced a two-step model reduction technique that combines the modeling versatility of the *ps*-FEM with the reduction in DOFs offered by the Rayleigh-Ritz method.

In the first step of this approach, the *ps*-FEM is used with a perturbation procedure to generate a subspace of global basis vectors. Two subspaces are proposed in this study, the first based on the path derivatives of static modes, the second on the path derivatives of buckling modes.

In the second step, the Rayleigh-Ritz method is employed to project the FE equations onto the reduced-basis subspace. The FE solution is approximated by a linear combination of a pre-selected set of global basis vectors. The size of the nonlinear FE is then reduced to few DOFs, corresponding to the Ritz amplitudes of the vectors composing the reduced subspace.

To further improve computational efficiency, the proposed model reduction technique has been coupled with a fast perturbation solution procedure, the ANM. Compared to classical IIPs, this approach allows for further computational saving, as fewer matrix factorizations and residual evaluations are needed.

The framework has been applied to the postbuckling analysis of a VS panel. The numerical results have shown that a ROM with barely a dozen DOFs can effectively predict the nonlinear prebuckling range, the limit point and the initial postbuckling response. In general, the moderate and deep postbuckling responses cannot be captured. Future investigations are directed toward the extension of the approach to overcome this latter restriction.

REFERENCES

[1] Sanchez-Majano, A., Pagani, A., Petrolo, M., and Zhang, C. 2021. "Buckling sensitivity of tow-steered plates subjected to multiscale defects by high-order finite elements and polynomial chaos expansion." Materials 14: 2706.
https://doi.org/10.3390/ma14112706

[2] Moreira, J. A., Moleiro, F., Araújo, A. L., and Pagani, A. 2023. "Assessment of layerwise user-elements in Abaqus for static and free vibration analysis of variable stiffness composite laminates." Composite Structures 303: 116291.
https://doi.org/10.1016/j.compstruct.2022.116291

[3] Iannotta, D. A., Giunta, G., and Montemurro, M. 2024. "A mechanical analysis of variable angle-tow composite plates through variable kinematics models based on Carrera's unified formulation." Composite Structures 327: 117717.
https://doi.org/10.1016/j.compstruct.2023.117717

[4] Wu, Z., Raju, G., and Weaver, P. M. 2013. "Postbuckling analysis of variable angle tow composite plates." International Journal of Solids and Structures 50, no 10: 1770-1780. https://doi.org/10.1016/j.ijsolstr.2013.02.001

[5] Hao, P., Liao, H., Wu, T., Huo, Z., and Wang, B. 2023. "Isogeometric degenerated shell formulation for post-buckling analysis of composite variable-stiffness shells." Composite Structures 321: 117209. https://doi.org/10.1016/j.compstruct.2023.117209

[6] Madeo, A., Groh, R. M. J., Zucco, G., Weaver, P. M., Zagari, G., and Zinno, R. 2017. "Post-buckling analysis of variable-angle tow composite plates using Koiter's approach and the finite element method." Thin-Walled Structures 110: 1-13. https://doi.org/10.1016/j.tws.2016.10.012

[7] Vescovini, R., Spigarolo, E., Jansen, E. L., and Dozio, L. 2019. "Efficient post-buckling analysis of variable-stiffness plates using a perturbation approach." Thin-Walled Structures 143: 106211. https://doi.org/10.1016/j.tws.2019.106211

[8] Liguori, F. S., Zucco, G., Madeo, A., Magisano, D., Leonetti, L., Garcea, G., and Weaver, P. M. 2019. "Postbuckling optimisation of a variable angle tow composite wingbox using a multi-modal Koiter approach." Thin-Walled Structures 138: 183-198. https://doi.org/10.1016/j.tws.2019.01.035

[9] Nagy, D. A., and König, M. 1979. "Geometrically nonlinear finite element behaviour using buckling mode superposition." Computer Methods in Applied Mechanics and Engineering 19, no 3: 447-484. https://doi.org/10.1016/0045-7825(79)90070-7

[10] Almroth, B. O., Stern, P., and Brogan, F. A. 1978. "Automatic choice of global shape functions in structural analysis." Aiaa Journal 16, no 5: 525-528. https://doi.org/10.2514/3.7539

[11] Noor, A. K., and Peters, J. M. 1981. "Bifurcation and post-buckling analysis of laminated composite plates via reduced basis technique." Computer Methods in Applied Mechanics and Engineering 29, no 3: 271-295. https://doi.org/10.1016/0045-7825(81)90046-3

[12] Chan, A. S. L., and Hsiao, K. M. 1985. "Nonlinear analysis using a reduced number of variables." Computer Methods in Applied Mechanics and Engineering 52, no 1-3: 899-913. https://doi.org/10.1016/0045-7825(85)90020-9

[13] Tao, D., and Ramm, E. 1991. "Characteristics of subspace in reduced basis technique." International Journal for Numerical Methods in Engineering 31, no 8: 1567-1583. https://doi.org/10.1002/nme.1620310809

[14] Kling, A., Degenhardt, R., and Zimmermann, R. 2006. "A hybrid subspace analysis procedure for non-linear postbuckling calculation." Composite Structures 73, no 2: 162-170. https://doi.org/10.1016/j.compstruct.2005.11.051

[15] Rahman, T., Ijsselmuiden, S. T., Abdalla, M. M., and Jansen, E. L. 2011. "Postbuckling analysis of variable stiffness composite plates using a finite element-based perturbation method." International Journal of Structural Stability and Dynamics 11, no 4: 735-753. https://doi.org/10.1142/S0219455411004324

[16] Liang, K., Sun, Q., and Zhang, Y. 2018. "Nonlinear buckling analysis of variable stiffness composite plates based on the reduced order model." Composite Structures 206: 681-692. https://doi.org/10.1016/j.compstruct.2018.08.092

[17] Zander, N., Bob, T., Kollmannsberger, S., Schillinger, D., and Rank. E. 2015. "Multi-level hp-adaptivity: High-order mesh adaptivity without the difficulties of constraining hanging nodes." Computational Mechanics 5: 499-517. https://doi.org/10.1007/s00466-014-1118-x

[18] Yan, C. A., and Vescovini, R. 2023. "Application of the ps-Version of the Finite Element Method to the analysis of laminated shells." Materials 16, no 4: 1395. https://doi.org/10.3390/ma16041395

[19] Yan, C. A., and Vescovini, R. 2024. "Asymptotic ps-FEM for nonlinear analysis of composite shells." International Journal of Mechanical Sciences 272: 109279. https://doi.org/10.1016/j.ijmecsci.2024.109279

[20] Cochelin, B., Damil, N., and Potier-Ferry, M. 1994. "The asymptotic-numerical method: an efficient perturbation technique for nonlinear structural mechanics." Revue Européenne des Eléments Finis 3, no 2: 281-297. https://doi.org/10.1080/12506559.1994.10511124

[21] Vescovini, R., Dozio, L., D'Ottavio, M., and Polit, O. 2018. "On the application of the Ritz method to free vibration and buckling analysis of highly anisotropic plates." Composite Structures 192: 460-474. https://doi.org/10.1016/j.compstruct.2018.03.017

[22] Babuska, I., Szabo, B. A., and Katz, I. N. 1981. "The p-version of the finite element method." SIAM Journal on Numerical Analysis 18, no 3: 515-545. https://doi.org/10.1137/0718033

[23] Mote Jr, C. D. 1971. "Global-local finite element." International Journal for Numerical Methods in Engineering 3, no 4: 565-574. https://doi.org/10.1002/nme.1620030410

[24] Cochelin, B., Damil, N., and Potier-Ferry, M. 1994. "Asymptotic–numerical methods and Pade approximants for non-linear elastic structures." International Journal for Numerical Methods in Engineering 37, no 7: 1187-1213. https://doi.org/10.1002/nme.1620370706